Surface Enhanced Raman Utilizing Magnetic Core Gold Shell Nanoparticles

K.J. Carroll[*], G. P. Glaspell,[*] N. McDowall, [*] L.W. Brown III,[*] K. Zhang, [**] A.K. Pradhan, [**] J. Anderson,[*] E.E. Carpenter[*]

[*] Department of Chemistry, Virginia Commonwealth University, Richmond, VA 23284, ecarpenter2@vcu.edu

[**]Center for Materials Research, Norfolk state University, Norfolk, VA 23504.

ABSTRACT

In this study, we investigate a novel two-step synthesis of $Fe/SiO_2/Au$ core/shell nanoparticles by aqueous reduction using sodium borohydride. The composition, morphology, and magnetic behavior were determined by X-ray diffraction, X-ray photoelectron spectroscopy, transmission electron microscopy, and room temperature vibrating sample magnetometry. We also demonstrate their application as surface-enhanced Raman substrates. We evaluate their performance as SERS active material using pyridine as a model compound. Core/shell nanoparticles with optical and magnetic functionality offer broad opportunities for biomedical and SERS applications.

Keywords: Nanoparticles, SERS, core/shell, etc

1 INTRODUCTION

Raman spectrometry has been successfully used for the identification and characterization of organic materials. However, due in part to the *low* scattering efficiency Raman spectroscopy has not been fully utilized in sensor applications. Surface enhanced Raman scattering (SERS) on the other hand has been shown to produce enhancement factors as high as 10^{14}-10^{15}, which is capable of detecting single molecules.[1] SERS is experiencing a resurgence of interest due in part to nanotechnology. Noble metal nanoparticles when excited develop a major surface plasmon along the surface of the particle resulting in enhanced Raman Scattering. The surface enhanced Raman (SER) effect is currently explained using chemical (CM) and electromagnetic (EM) mechanisms.[2] Chemical effects provide enhancement via an increase in the molecular polarizability of the adsorbate due its interaction with the metal surface. Maximum chemical enhancement is observed when the substrate forms a monolayer on the metal of interest. This phenomenon can be modulated by molecules adsorbed on the surface allowing for the development of sensors. As opposed to other sensors where specific moieties on the analyte contribute to the signal, with SERS each different type of moiety would allow for a different modulation of the SERS thus allowing for simultaneous detection of different analytes. Furthermore, SERS is capable of identifying structural features of various analytes.

Kneip and coworkers have shown that SERS spectra of various analytes were measured down to 10^{-7} M (this corresponds to a sensitivity of less than 1 pg) in colloidal gold solutions. Nie has also shown that not all particles are SER active and have reported that the aggregation of individual particles can lead to intense SER enhancement through the formation of ‘‘hot spots’’ (an intense plasmon resonance that exists between two particles in close proximity).[1] A ‘‘hot spot’’ can provide enhancement factors as high as 10^{13} to 10^{14}; sensitive enough for single molecule detection. A coupling of the particle resonances and the confined region between particles causes the observed enhancement. It is therefore possible that inducing a magnetic field may also create hotspots between adjacent nanoparticles further enhancing their sensitivity.

The last several years have seen an increasing interest in designing nanoparticles with multifunctional properties. Over the past year, nanoparticles have been designed such that they combine both optical and magnetic properties with promising applications to biomedical, engineering, and sensor design.[3-8] Specifically, Kim and coworkers for the first time claim to have designed a novel one step synthesis of $Ag@Fe_2O_3$ nanoparticles specifically for SERS-based detection of chemical species.[8] In their process, they synthesize Fe_2O_3 nanoparticles and then redisperse them for silver coating. We however report on $Fe/SiO_2/Au$ core/shell nanoparticles by aqueous reduction using sodium borohydride. The concept of utilizing a SiO_2 shell may isolate the Au from any possible interference due to the Fe core.

Raman spectroscopy is capable of providing a “fingerprint” by which molecules can be identified; the signals are often too weak to be practical for sensor applications. We propose coupling the surface enhancement observed with noble metals with the magnetic properties of an iron core. The magnetic core provides the capability to recollect distributed sensors after attachment of the target molecule, thereby concentrating the molecules of interest and increasing detection sensitivity. Since Raman spectroscopy utilizes vibrational modes that are specific to individual molecules, we believe that we should be able to identify various analytes of interest on the nanoparticle surface.

2 SYNTHESIS AND CHARACTERIZATION

2.1 Synthesis of Fe NPs

Fe NPs were synthesized by using a previously reported procedure.[9-10] Typically, 4.6 mM of iron (II) sulfate heptahydrate and 0.46 mM trisodium citrate dihydrate were added to 2L of DI-H_2O under magnetic stirring in a 4L Erlenmeyer flask at room temperature. The mixture was allowed to stir for 5 minute to ensure dissolution. Then, 1.56 g of sodium borohydride was added and allowed to stir for 10 minutes. The solution was quenched with ethanol several times and magnetically separated using a rare-earth magnet. After washing, the remaining ethanol was decanted and the particles were placed in a vacuum oven at room temperature to dry.

2.2 Synthesis of Fe@SiO_2 NPs

A total of 1.50 g of Fe NPs were added to 20 mL of DI-H_2O and 200 mL ethanol under magnetic stirring in an Erlenmeyer flask. Then 1 mL of TEOS was slowly added for 30 minutes using an addition funnel and then allowed to react for 6 hours.

2.3 Synthesis of Fe@SiO_2@Au NPs

To the Fe@SiO_2 NP solution 1 mL of 0.490 M $HAuCl_4$ was added. Then 0.204 g of sodium borohydride was added to the solution and the reaction was allowed to react for 10 minutes. The solution was quenched with ethanol several times and magnetically separated. After washing the particles were placed in a vacuum oven at room temperature to dry prior to analysis.

2.4 Heat Treatment

The dried Fe@SiO_2@Au nanoparticles were heated in an oven under N_2 atmosphere to 400 °C for 30 minutes with a 10 °C/min ramp rate.

2.5 Characterization

Microstructure analysis of the NPs was conducted using high-resolution transmission electron microscopy. HRTEM analysis was performed on the nanoparticles with a field-emission transmission electron microscope (TEM, JEOL, JEM 2010, accelerating voltage 200 KV). The nanoparticles were sonicated and vacuum dried on the copper grid before placing in the TEM chamber. The crystal structures were analyzed by a X-ray diffraction (XRD) spectrometry (Panalytical X'pert pro) equipped with a Cu Kα radiation source (λ=0.15406 nm).

For X-ray photoelectron spectroscopy (XPS) analysis, the samples were transferred to the sample chamber of a Thermo Scientific ESCALAB 250 microprobe with a focused monochromatic Al Kα radiation source (E_b= 1486.6 eV). The depth profiling experiments were conducted with a high energy Ar^+ ion beam. All XPS spectra were referred by aliphatic C 1s (284.5 eV). The magnetic properties were measured at room temperature using a Lakeshore Cryotonics Inc. Model 7300 VSM.

3 RESULTS AND DISCUSSION

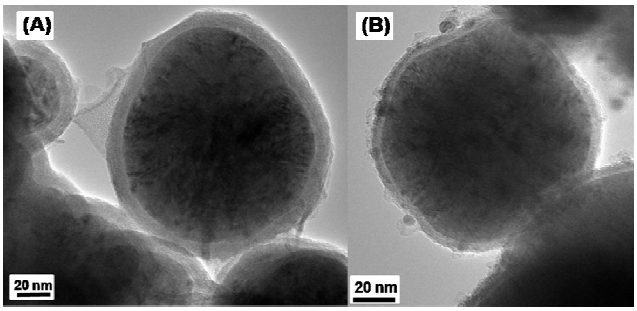

Figure 1. TEM images of (A) Fe/SiO_2 nanoparticles and (B) Fe/SiO_2/Au nanoparticles.

Figure 1 shows typical TEM images of the as-prepared 80 nm Core/shell Fe/SiO2 NPs with the iron core being 75 nm and the SiO_2 shell being 5 nm and the Fe/SiO_2/Au NPs with Au islands of 4-5 nm.

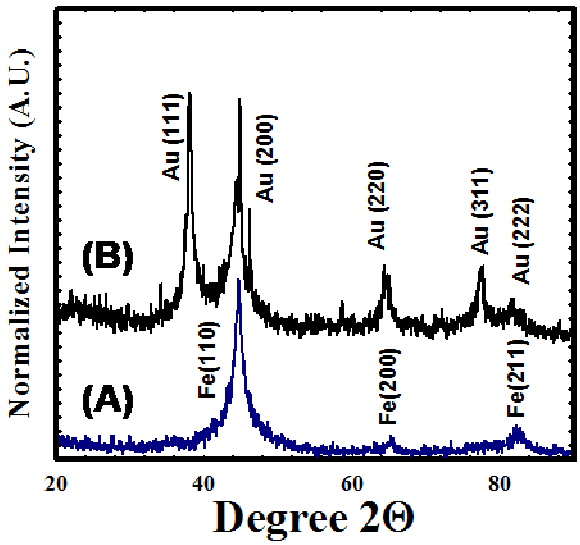

Figure 2. XRD patterns of (A) as-synthesized Fe/SiO_2 nanoparticles and (B) as-synthesized Fe/SiO_2/Au nanoparticles.

The XRD patterns of the as-prepared core/shell nanoparticles are presented in figure 2. All the diffraction peaks of Au can be indexed to face-centered cubic (fcc) crystal structure while the Fe can be indexed to body centered cubic (bcc). In the figure, the data is presented with the miller indices from the JCPDS reference powder diffraction files α-Fe (01-089-7194) and Au (01-04-0784). From the diffraction data, it can be seen that there are no Fe oxide impurities.

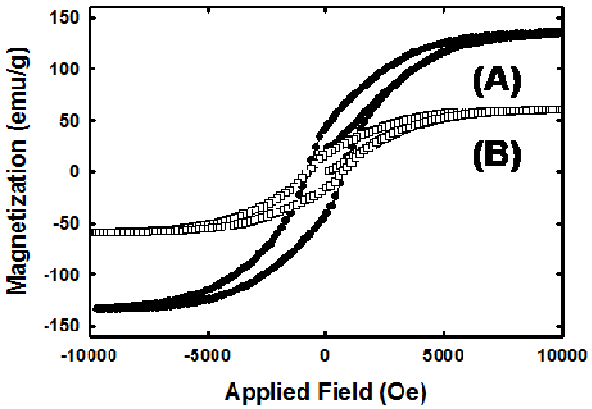

Figure 3. Room temperature Hysteresis loops for (A) as-synthesized Fe nanoparticles and (B) as-synthesized $Fe/SiO_2/Au$ nanoparticles.

Room temperature hysteresis loops are shown in figure 3. The as-synthesized saturation magnetizations Fe and $Fe/SiO_2/Au$ nanoparticles were found to be 148 emu/g and 58 emu/g, respectively. From the TGA data (Figure 4) it can be seen that roughly 10 percent of unreacted citrate is adsorbed onto the Fe/SiO2/Au nanoparticles and using a mass correction the corrected magnetization was calculated to be roughly 69 emu/g.

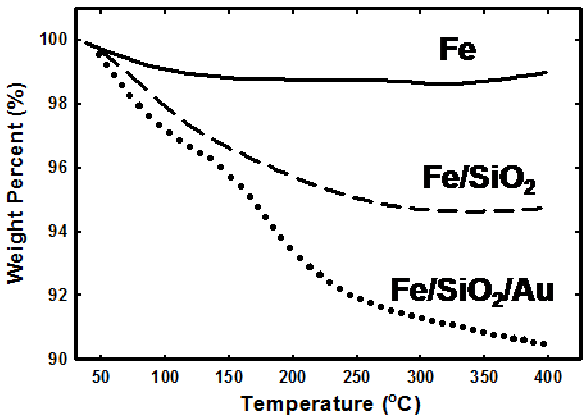

Figure 4. TGA analysis of Fe, $FeSiO_2$, and $Fe/SiO_2/Au$ nanoparticles.

Using the TGA the Fe/SiO2/Au samples were heat treated to 400 °C using N_2 gas. As mentioned above, about 10 percent weight loss was seen when the samples were heated. It is hypothesized that this reduction is due to the loss of organics that were adsorbed onto the surface of the particles along adsorbed H_2O.

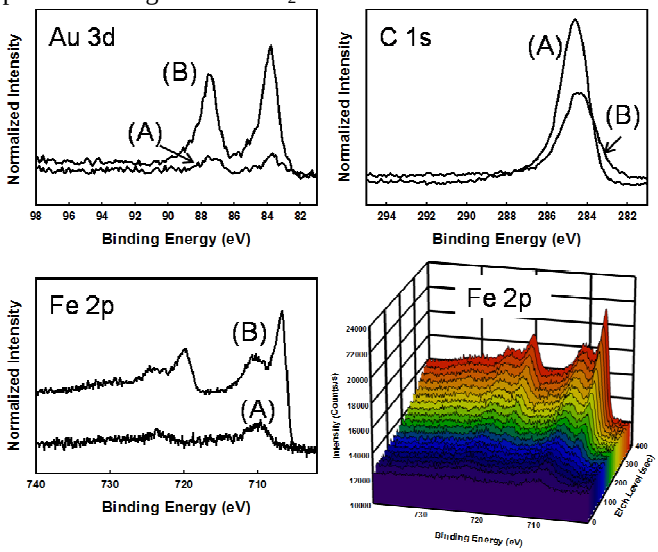

Figure 5. XPS spectra of before (A) and after (B) annealing of $Fe/SiO_2/Au$ nanoparticles.

To confirm this XPS analysis was conducted on the pre- and post- annealed samples. Figure 5 depicts the results of the XPS analysis. From the C 1s spectrum a decrease in the intensity of the C-C peak is seen after the samples are annealed under N_2 gas. This decrease is coupled with an increase in the intensity of the Au 3d peak, which supports the hypothesis that organics were on the surface obstructing the Au surface. In addition, an increase in the Fe 2p peak is seen. A high-resolution depth profile analysis shows that as the sample is etched the intensity of the Fe 2p increases. More importantly, an increase in the metallic Fe (BE=709 eV) peak correlates with the XRD analysis.

The aggregation of nanoparticles occurs naturally in solution due in part to the reduced surface energy after aggregation, it is also possible by utilizing magnetic fields and magnetic nanoparticles. While it is difficult to collect SERS on magnetic nanoparticles consisting solely of Fe, Co or Ni, it becomes possible with core-shell nanoparticles. To test this hypothesis, we show through experimentation that by utilizing the $Fe/SiO_2/Au$ core/shell nanoparticles the nanoparticles can be concentrated along magnetic field gradients which offers the distinct advantage of piloted movement of the target analyte. The observed SERS enhancement could arise from a combination of two particular scenarios (Figure 6 A). The first scenario is indicative of the analyte of interest localized by the magnetic field providing an increase in the observed Raman signal. The other scenario is related to the aggregation of gold particles. The aggregation of gold particles leads to "hot spots" showing increased SERS response.

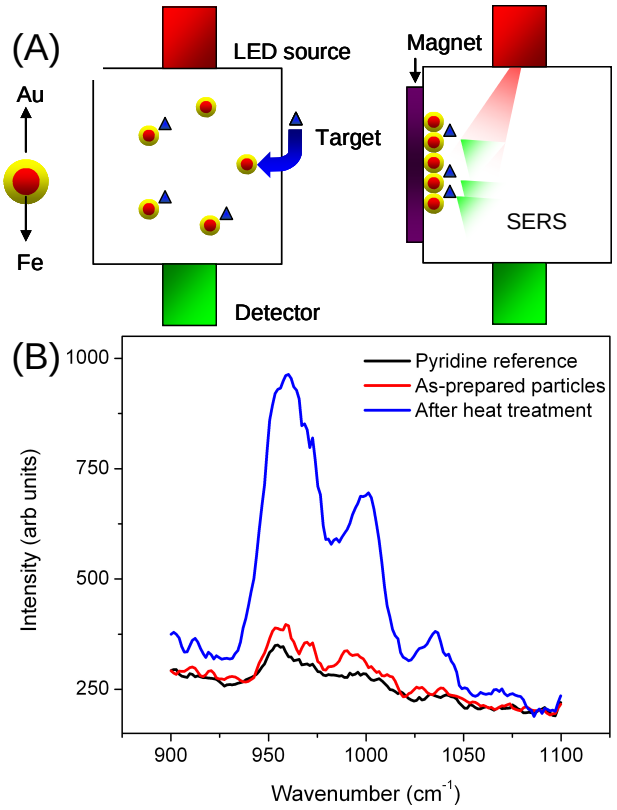

Figure 6. (A) Utilizing magnetic core shell particle to pre-concentrate the target analyte for improved sensitivity. (B) SERS of the pyridine reference and $Fe/SiO_2/Au$ core/shell nanoparticles before and after heat treatment. The SERS is dominated by two intense bands at about 1,008 and 1,036 cm^{-1}, corresponding to the ring breathing and to the triangular-deformation modes, respectively.

In order to determine the affect of magnetic pre-concentration on the SERS response, we collected Raman spectra of pyridine, a compound commonly used in SERS studies, using a Raman Systems R-3000 spectrometer equipped with a 785 nm laser. The pyridine solution also contained 5 ml of ethanol which served as our internal intensity standard. In a typical experiment, magnetic SERS particles were then added to the standard pyridine solution and left to set for up to 20 minutes. In the presence of an external magnetic field all the particles were collected to one side of a cuvette and the SERS spectra was collected and is indicated in Figure 6. It is significant to note that the Raman spectra of the heat treated particles did in fact increase after the magnetic field was applied. Previously we alluded to two possible scenarios for enhancement. First, pyridine is chemisorbed onto the modified magnetic particles and after the magnetic field is applied the increased signal is proportional to the higher concentration of localized pyridine. Secondly, the increased SERS signal stems from "hot spots" generated by the aggregation of the modified magnetic particles. Since we are using a 785 nm laser which is somewhat removed from the plasmon resonance of the gold surface, typically around 520 nm, it is reasonable to assume the first scenario likely holds true. Future experiments will incorporate the use of Nd:YAG, 532 nm, which operates closer to the plasmon resonance of gold in order to determine if "hot spots" are indeed forming.

4 CONCLUSION

In conclusion, we reported on a novel two-step synthesis of $Fe/SiO_2/Au$ core/shell nanoparticles by aqueous reduction using sodium boroydride. Based on TEM, XRD, XPS, and TGA characterization, we demonstrated that the as prepared particles are not SERS active and require heat treatment to remove citrate from the surface. We have also demonstrated using Raman spectroscopy that after heat treatment the nanoparticles are SERS-active and show practical applications, including piloted movement of absorbed analytes, for SERS based detection.

5 ACKNOWLEDGEMENTS

The authors would like to thank the VCU nanomaterials core characterization facility for instrument time as well as the NSF MRI grant CHE-0820945.

6 REFERENCES

[1] Nie, S.; Emory, S. R. *Science* **1997**, *275*, 1102.

[2] Glaspell, G. P.; Zuo, C.; Jagodzinski, P. W. *Journal of Cluster Science* **2005**, *16*, 39.

[3] Levin, C. S.; Hofmann, C.; Ali, T. A.; Kelly, A. T.; Morosan, E.; Nordlander, P.; Whitmire, K. H.; Halas, N. J. *ACS Nano* **2009**, *3*, 1379.

[4] Radwan, F. R.; Carroll, K. J.; Carpenter, E. E. *J. Appl. Phys.* **2009**, *in press*.

[5] Wang, H.; Brandl, D. W.; Le, F.; Nordlander, P.; Halas, N. J. *Nano Letters* **2006**, *6*, 827.

[6] Noh, M. S.; Jun, B.-H.; Kim, S.; Kang, H.; Woo, M.-A.; Minai-Tehrani, A.; Kim, J.-E.; Kim, J.; Park, J.; Lim, H.-T.; Park, S.-C.; Hyeon, T.; Kim, Y.-K.; Jeong, D. H.; Lee, Y.-S.; Cho, M.-H. *Biomaterials* **2009**, *30*, 3915.

[7] Jun, B.-H.; Noh, M. S.; Kim, J.; Kim, G.; Kang, H.; Kim, M.-S.; Seo, Y.-T.; Baek, J.; Kim, J.-H.; Park, J.; Kim, S.; Kim, Y.-K.; Hyeon, T.; Cho, M.-H.; Jeong, D. H.; Lee, Y.-S. *Small* **2009**, *9999*, NA.

[8] Kim, K.; Jang, H. J.; Shin, K. S. *Analyst* **2009**, *134*, 308.

[9] Carroll, K. J.; Pitts, J. A.; Zhang, K.; Pradhan, A. K.; Carpenter, E. E. *J. Appl. Phys.* **2010**, accepted.

[10] Carroll, K. J.; Hudgins, D. M.; Brown, L. W.; Yoon, S. D.; Heiman, D.; Harris, V. G.; Carpenter, E. E. *J. Appl. Phys.* **2010**, accepted.